



Article

Study of the Dissolution and Diffusion of Propane, Propylene and Nitrogen in Polydimethylsiloxane Membranes with Molecular Dynamics Simulation and Monte Carlo Simulation

Weibin Cai ¹ , Mingqian Wang ¹, Gary Q. Yang ^{2,*} , Zhijun Zhang ¹, Yujun Wang ³ and Jiding Li ³

¹ School of Chemical and Environmental Engineering, China University of Mining and Technology, Beijing 100083, China; caiweibin@tsinghua.org.cn (W.C.); 18852140162@163.com (M.W.); zhangzjchem@cumtb.edu.cn (Z.Z.)

² College of Bioscience and Bioengineering, Jiangxi Agricultural University, Nanchang 330045, China

³ Department of Chemical Engineering, Tsinghua University, Beijing 100084, China; wangyujun@tsinghua.edu.cn (Y.W.); lijiding@tsinghua.edu.cn (J.L.)

* Correspondence: materialresearch@sina.com

Abstract: Volatile organic compounds (VOCs) are important sources of atmospheric pollutants on account of their high recycling value. The membrane of dense silicone rubber polydimethylsiloxane (PDMS) has wide-ranging prospects for the separation and recovery of VOCs. In this study, PDMS membrane body models were established in BIOVIA Materials Studio (MS) to simulate VOCs with C₃/N₂ gases, and to study the structure of PDMS membranes and the dissolution and diffusion process of gas in the membranes. The free volume fraction (FFV), cohesive energy density (CED), radial distribution function (RDF), diffusion coefficient and solubility coefficient of C₃H₈, C₃H₆ and N₂ in PDMS membranes were calculated, and the permeability coefficients were calculated according to these values. At the same time, the effects of temperature and mixed gas on the dissolution and diffusion of C₃/N₂ in PDMS membranes were investigated. The results show that the mass transfer process of C₃ in PDMS membranes is mainly controlled by the dissolution process, while that of N₂ is mainly controlled by the diffusion process. In a C₃/N₂ mixed gas system, there is a synergistic relationship between gases in the diffusion process, while there is competitive adsorption in the dissolution process. With an increase in temperature, the diffusion coefficients of the three gases in PDMS gradually increase, the solubility coefficients gradually decrease, and the overall permeability selectivity coefficients of the gases gradually decrease. Therefore, low-temperature conditions are more conducive to the separation of C₃/N₂ in PDMS membranes. The simulation results of the permeability selectivity coefficients of pure C₃ and N₂ in PDMS are similar to the experimental results, and the relationship between the micro- and macro-transport properties of PDMS membranes can be better understood through molecular simulation.

Keywords: PDMS; molecular dynamics simulation; monte carlo simulation; volatile organic compounds (VOCs)



Citation: Cai, W.; Wang, M.; Yang, G.Q.; Zhang, Z.; Wang, Y.; Li, J. Study of the Dissolution and Diffusion of Propane, Propylene and Nitrogen in Polydimethylsiloxane Membranes with Molecular Dynamics Simulation and Monte Carlo Simulation. *Separations* **2022**, *9*, 116. <https://doi.org/10.3390/separations9050116>

Academic Editor: Barbara Bojko

Received: 1 April 2022

Accepted: 8 May 2022

Published: 10 May 2022

Publisher's Note: MDPI stays neutral with regard to jurisdictional claims in published maps and institutional affiliations.



Copyright: © 2022 by the authors. Licensee MDPI, Basel, Switzerland. This article is an open access article distributed under the terms and conditions of the Creative Commons Attribution (CC BY) license (<https://creativecommons.org/licenses/by/4.0/>).

1. Introduction

With the large-scale development of modern industry, environmental problems and the energy crisis are becoming more and more serious. Volatile organic compounds (VOCs) are important atmospheric pollutants. VOCs have complex components and a wide range of sources [1,2]. VOCs come from anthropogenic emissions and natural emissions. In recent years, industrial emissions have accounted for an increasing proportion of VOCs [3]. VOCs from industry generally have irritant and toxic effects, and are seriously harmful to human health [4,5]. They are also flammable and explosive, rendering production and transportation dangerous [6,7]. Although VOCs are generally harmful, they can be valuable. In petroleum refining, the organic chemical industry and other industries, VOCs contain a

large number of recyclable light hydrocarbons, such as propylene and propane. Recycling hydrocarbons not only reduces environmental pollution, but also brings about economic benefits [8]. Propylene and propane are rather extensively observed VOCs. Exploring them provides us with general information on VOCs. It is more suitable to choose propylene and propane over other light hydrocarbons, such as methane, which is too simple and, therefore, unsuitable as a general representative of VOCs.

Organic vapor membrane separation technology is a new type of VOC recovery technology. It is suitable for nearly all kinds of VOCs, and has the advantages of a high recovery rate, low energy consumption, no secondary pollution, etc. [9–12]. The VOC mixture first dissolves on the membrane surface at the feed side. The components adsorbed on the membrane surface diffuse through the membrane and desorb on the membrane surface at the permeation side. VOCs can penetrate the membrane and are enriched on the permeation side, while air and other gases that have difficulty penetrating the membrane are enriched on the feed side. As such, the mixtures are separated and purified using the technology [13].

Compact silicone rubber polydimethylsiloxane (PDMS) has been widely used for its high gas permeability. Sahin et al. [14] separated organic vapor from N_2 by filling PDMS membranes with a zeolite imidazolate framework (ZIF). Gazic et al. [15] prepared different polymer membranes to recover 1-ethyl-2-methylbenzene from aqueous solutions by pervaporation, and found that PDMS membranes had the highest total flux. Kim et al. [16] prepared PDMS membranes with PEG-impregnated non-woven fabric as a support layer to separate VOCs mainly composed of toluene. Shi et al. [17] used a PDMS composite membrane for the separation of C_3H_6 and N_2 ; they found that PDMS membranes can effectively separate C_3H_6 from N_2 and verified the feasibility of PDMS membranes for olefin recovery in polyolefin purge gas.

According to previous experimental results [18], we know that C_3H_8 and C_3H_6 have a higher transport rate than N_2 in PDMS, though N_2 has a smaller volume than C_3H_8 and C_3H_6 . To explain this unusual phenomenon, we need to explore gas transport in PDMS at the molecular level and obtain profound knowledge of this process. Molecular dynamics (MD) simulations have been widely used by researchers to explore such mechanisms at the molecular level. Liu et al. [19] simulated the mass transfer process of furfural and water in polyether block amide (PEBA-2533) membranes, revealing the influence of membrane structure on selectivity at the molecular level. Pazirotteh et al. [20] studied the structure, transport mechanism and properties of two polyether block amide membranes in the presence of functional nanoparticles using a molecular dynamics (MD) simulation and found that the simulation results were essentially consistent with the experimental results, proving that MD simulation yields rather precise results. Wang et al. [21] studied the swelling behavior of PEBA-2533 membranes in aqueous solutions of phenol, aniline and furfural through experiments and MD simulation, and analyzed the effects of non-bond interaction energy and hydrogen bond number between water and high boiling point organic compound (HBOC) molecules on the swelling degree of PEBA-2533. Molecular simulation technology can be used not only to explore the dissolution and diffusion mechanism of permeation at the molecular level, but also to provide precise values for various macro physical property data. Therefore, we carried out MD simulations of gas transport in PDMS.

In this study, using BIOVIA Materials Studio (MS, Accelrys Software Inc. San Diego, USA), we simulated gas transport in PDMS membranes. The dissolution and diffusion properties of three different gases (C_3H_8 , C_3H_6 , and N_2) were simulated and analyzed in the membranes at different temperatures. We were then able to ascertain the factors that lead to this unusual phenomenon. The differences in mass transfer processes between mixed gases and pure gases in PDMS membranes were also investigated. In addition, a series of properties, such as the free volume fraction, the cohesive energy density, the density field distribution and the adsorption energy distribution of the membranes, was also studied.

2. Models and Methods

The MD simulations were carried out using MS software. The COMPASS force field was used, the electrostatic interaction was calculated using the Ewald summation method and the van der Waals interaction, and the Supplementary Materials (SM) was computed by selecting the “atom-based” option [19,21]. The structures of C_3H_8 , C_3H_6 , N_2 and the PDMS monomer were drawn by the “visualizer” module. Firstly, relaxation and optimization were performed on these structures. PDMS chains composed of 50 repeating monomers were constructed using the “homopolymer” module.

Then, the initial models of the membranes were established using the “amorphous cell” module. The lattice type was set as cubic, and the final density of the cell was set as 0.97 g/cm^3 . The output was 10 cells. In order to prevent any interaction between the polymer chains, only one chain was placed in each cell, and the cells initially had a low density (0.1 g/cm^3). The cells with the lowest energy were selected for further optimization. Different gas molecules were loaded into PDMS cells to obtain simulation systems for each gas. A total of five gas molecules were put into each model. For the model of mixed gas, one N_2 molecule and four C_3 molecules were put into each system. Then, the “smart minimizer” method was used to minimize the system energy and relax the structures. For the minimization process, the convergence level was set to $0.001 \text{ kcal mol}^{-1} \text{ \AA}$. Afterwards, the cells were annealed in the “anneal” module, gradually heated from 200 K to 600 K, and then cooled to 200 K again. The process was repeated five times. With high-temperature relaxation, the distribution of holes was closer to that of the real material. Then, 100 ps MD simulations were performed successively in the NVT ensemble and the NPT ensemble at 298 K for the final optimization. The structures of the membrane cells are presented in Figure 1.

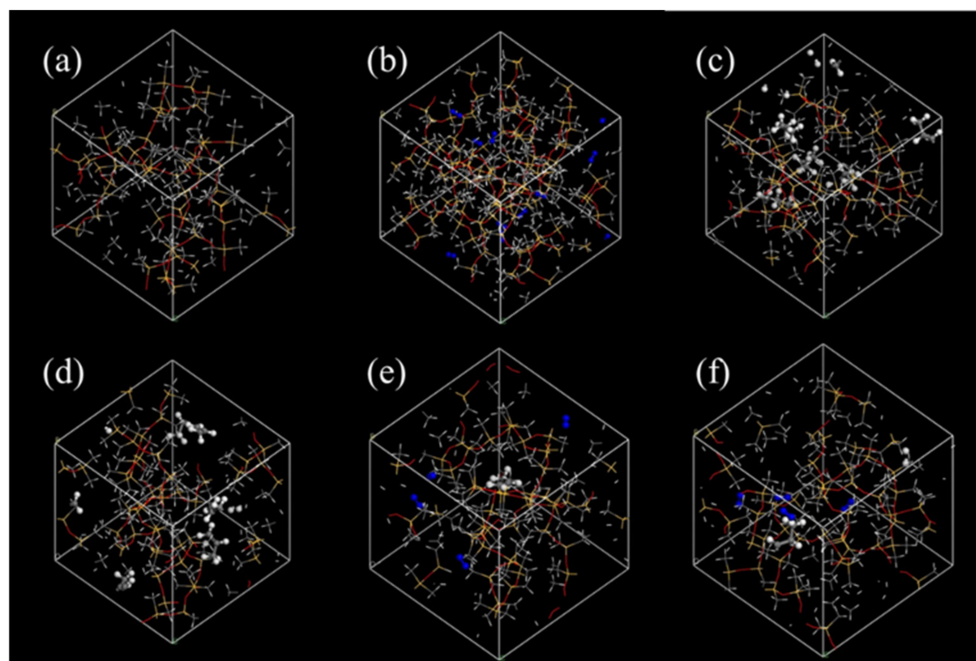


Figure 1. Structures of the membrane cells of (a) PDMS, (b) PDMS + N_2 , (c) PDMS + C_3H_8 , (d) PDMS + C_3H_6 , (e) PDMS + C_3H_8/N_2 and (f) PDMS + C_3H_6/N_2 .

Through an analysis of the optimization model, the characteristic parameters of the membrane can be obtained, such as the fraction of accessible volume (FAV), the cohesive energy density (CED) and the radial distribution function (RDF). Part of the PDMS membrane volume is occupied by molecular chains, and the other part is free volume. FAV represents the percentage of free volume available in the membrane relative to the total volume of the membrane. The CED is used to characterize the intermolecular force of polymers and judge

the stacking degree of chain segments. The RDF reflects the aggregation characteristics between atoms or molecules.

The optimized model was used for GCMC simulation and MD simulation to study the dissolution and diffusion process of molecules in the model. The solubility coefficient and the diffusion coefficient of different gas molecules in the PDMS membrane were calculated, and the permeability coefficient was then calculated. The permeability coefficient indicates how difficult it is for gas molecules to pass through the polymer membrane.

The SM presents the relevant knowledge and calculation techniques of the FAV, the CED, the RDF, the diffusion coefficient, the solubility coefficient and the permeability coefficient.

3. Results and Discussion

Table 1 shows the calculated CED values of PDMS from the MD simulation results and the CED values of PDMS in the literature. The simulation value of PDMS is close to the literature value, which shows that the construction of the model is reasonable.

Table 1. CED values of PDMS.

	Simulation Value	Literature Value
CED ($10^7 \text{ cal}\cdot\text{m}^{-3}$)	5.46	5.33 [22] 6.61 [23] 4.23 [24] 5.35 [25]

To obtain profound knowledge of gas transport in PDMS, we studied the distribution of free volume and accessible volume in PDMS simulation cells, because gas molecules can only diffuse in accessible free volume.

Figure 2 shows the accessible spaces determined by setting a different Connolly radius for the probes. Table 2 shows the free volume, occupied volume, total volume and FAV determined by probes with a different radius. The FFV of the PDMS membrane is 44.62%, which is larger than that of most polymers, including polyethylene and polypropylene. According to the figures, with a gradual increase in the probe radius, some accessible spaces shrink and finally disappear. As the radius of N_2 molecules (1.8 \AA) was used as the probe size, the FAV in PDMS reached 24.24%. However, when the radius of C_3 molecules (2.2 \AA) was used as the probe size, the FAV decreased to 16.48%. As a result, the N_2 molecules had more space to pass through the PDMS membrane than the C_3 molecules. It appears that in the PDMS membrane, N_2 molecules have a higher transport rate than C_3 molecules.

Then, the RDF of PDMS membrane atoms was calculated. The results are presented in Figure 3. Figure 3a shows the RDF of all the atoms of the PDMS. It is observed that the atoms of the PDMS lack long-range order, indicating that the polymer is amorphous. As the distance is shorter than 1 \AA , the peak intensity is zero, indicating that the distance between the atoms is larger than 1 \AA , which reflects the mutual repulsive force between the atoms. Figure 3b shows the RDF between the Si atoms and the C atoms of the branch chain. The radial distribution between the C atoms and the Si atoms has a sharp peak at 2.25 \AA . This is the bond length of the C-Si bond.

A mean square displacement (MSD) curve can be used to calculate the diffusion coefficient. Over long time intervals, when ions enter the Fickian diffusive zone, the MSD values are linear over time. Figure 4 shows the MSD values as a function of time for the transport of gases in PDMS membranes at 298 K. According to the MSD-t curve obtained from the simulation analysis, the logarithmic curve of MSD-t is drawn and fitted linearly. The region corresponding to the part with the slope of a logarithmic curve of about one is the normal diffusion region, and the diffusion coefficient can only be calculated by MSD in the normal diffusion region. For all gases, the normal diffusion region is reached within 1200 ps.

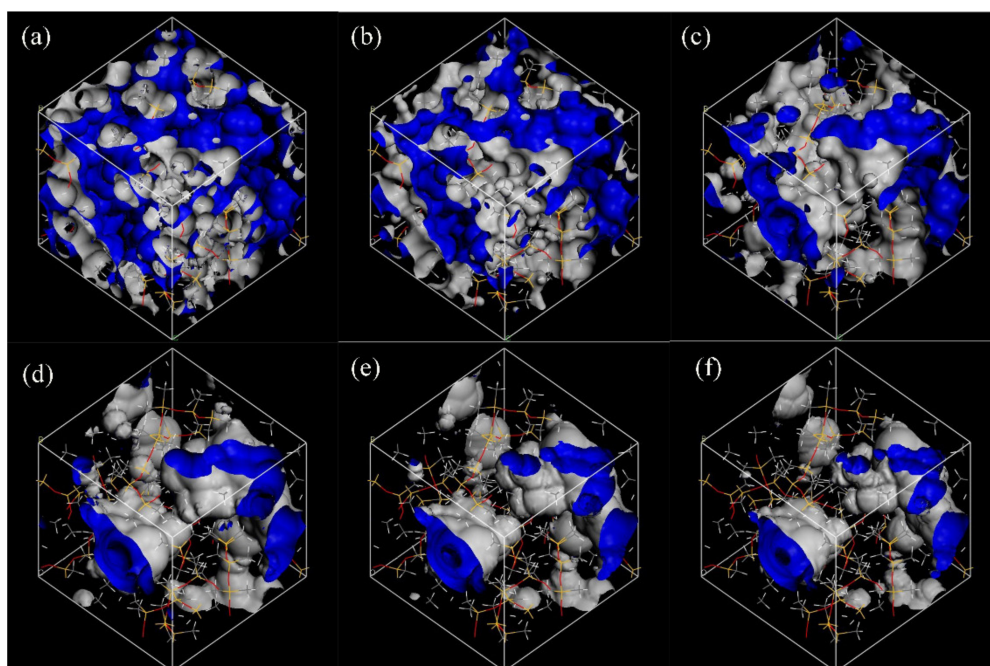


Figure 2. Accessible spaces determined by setting different Connolly radiuses for the probes: (a) 0 Å, (b) 0.5 Å, (c) 1 Å, (d) 1.8 Å, (e) 2.2 Å, and (f) 2.5 Å (blue and white represent the free volume field).

Table 2. Volume parameters measured by probes with a different radius (the total volume is 6350.65 Å³).

Connolly radius/Å	0	0.5	1	1.8	2.2	2.5
Free volume/Å ³	2833.85	2529.03	1996.74	1315.62	1046.66	869.79
Occupied volume/Å ³	3516.80	3821.62	4353.91	5035.03	5303.99	5480.86
FAV/%	44.62%	39.82%	31.44%	20.72%	16.48%	13.70%

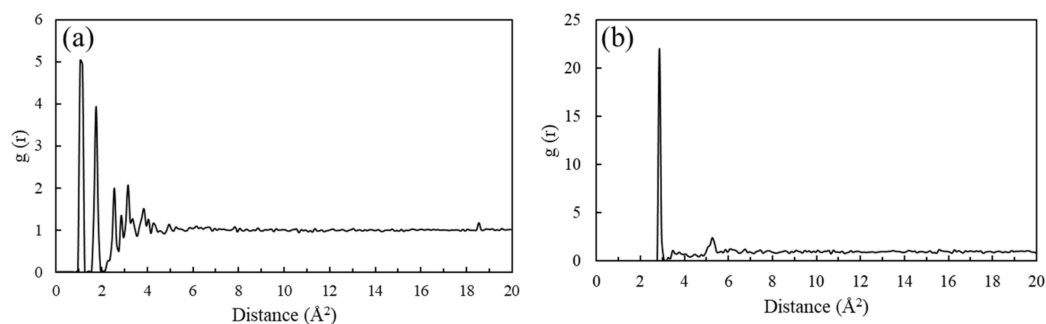


Figure 3. (a) RDF of all the atoms of the PDMS membrane and (b) RDF between Si atoms on the main chain and C atoms on the branch chain.

The slope of the MSD-t curve of N₂ is much larger than those of C₃H₈ and C₃H₆; the slopes of C₃H₈ and C₃H₆ are close to each other. As a result, the diffusion coefficients of N₂ are much greater than those of C₃ molecules, and the diffusion coefficients of the two C₃ gases are similar to each other, which is consistent with the FAV results. Therefore, smaller molecules show larger diffusivities.

Table 3 shows the diffusion coefficients of C₃/N₂ as pure gases and mixed gases in PDMS. The diffusion coefficients of various gases in the mixed gas systems are higher than those of pure gases. The diffusion coefficients of N₂ in both systems are much greater than those of both C₃ molecules. The increase in N₂ diffusion coefficients in the mixed gas system is smaller than those of both C₃ molecules in mixed gas systems, indicating that mixing N₂ with other gases has a relatively smaller influence on the diffusion of N₂.

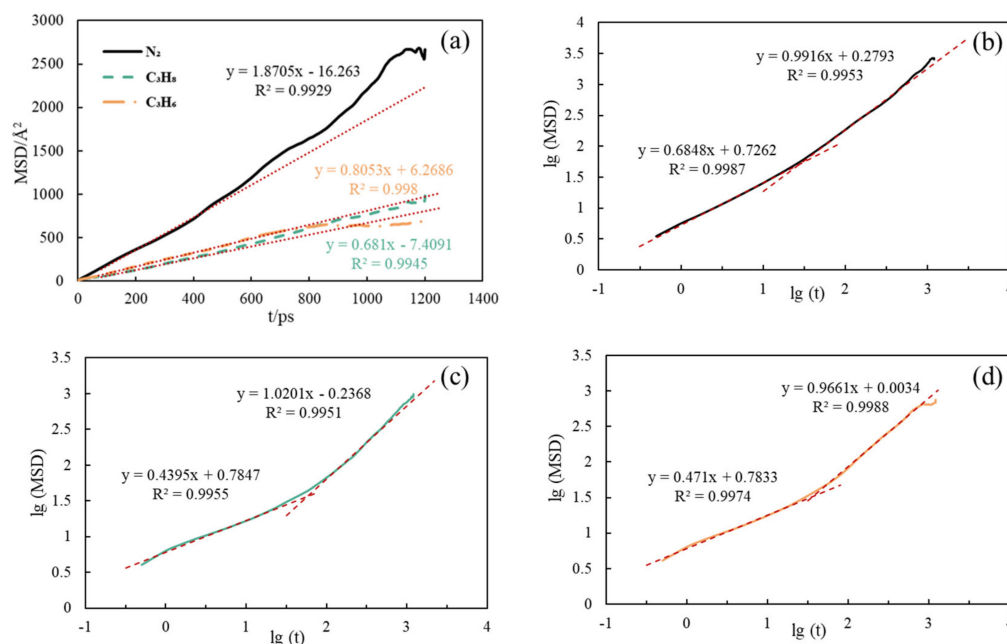


Figure 4. The MSD–t curve for the transport of C₃/N₂ (a) and the lg (MSD) –lg (t) curve for the transport of N₂ (b), C₃H₈ (c) and C₃H₆ (d).

Table 3. Diffusion coefficients of C₃/N₂ as (a) pure gases and (b) mixed gases in PDMS.

Pure Gas	D × 10 ⁴ /cm ² ·s ⁻¹	Mixed Gas	D × 10 ⁴ /cm ² ·s ⁻¹
N ₂	3.117	N ₂	3.243
C ₃ H ₈	1.134	C ₃ H ₈	1.975
C ₃ H ₆	1.342	C ₃ H ₆	1.980

Figure 5 shows the diffusion coefficients of N₂, C₃H₈ and C₃H₆ in the PDMS membrane at temperatures of 288 K, 298 K, 308 K, 318 K and 328 K. With a temperature increase from 288 K to 328 K, the diffusion coefficients gradually increase as well. Equation (1) is based on the Arrhenius formula [26]:

$$D = D_0 \exp\left(-\frac{Q}{RT}\right) \tag{1}$$

where D_0 is the diffusion constant, Q is the diffusion activation energy, R is the gas constant and T is the temperature. It is generally believed that D_0 and Q are independent of temperature. Therefore, when T increases, D will also increase. The simulation results are in line with this trend.

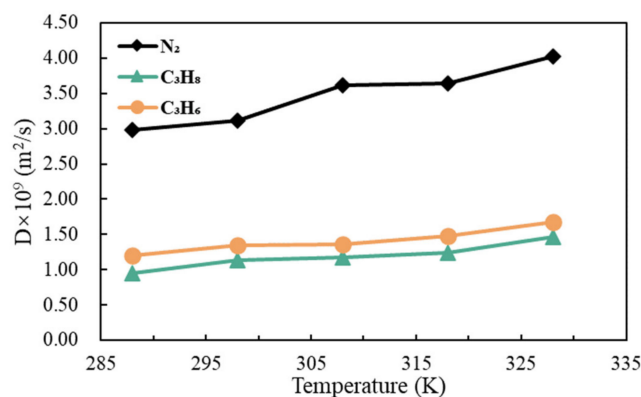


Figure 5. Diffusion coefficients of C₃/N₂ in PDMS membranes at different temperatures.

It can also be observed from Figure 5 that at the same temperature, the larger the gas molecule, the smaller the diffusion coefficient. This phenomenon can be explained by the free volume of the membrane. N_2 has more holes to pass through the membrane than C_3 , so it has a higher diffusion coefficient.

Figure 6 shows the trajectories of the three gases at 298 K. The gases jump among holes in PDMS in the diffusion process. The space ranges that gases reach are determined by the magnitudes of the diffusion coefficients. The diffusion range of N_2 is larger than that of C_3 . Because the volume of N_2 molecules is smaller, they can reach some holes with a volume smaller than that of C_3 molecules, and the diffusion coefficient of N_2 is larger than that of C_3 , that is, N_2 has a higher diffusion rate. Therefore, N_2 has the largest diffusion range.

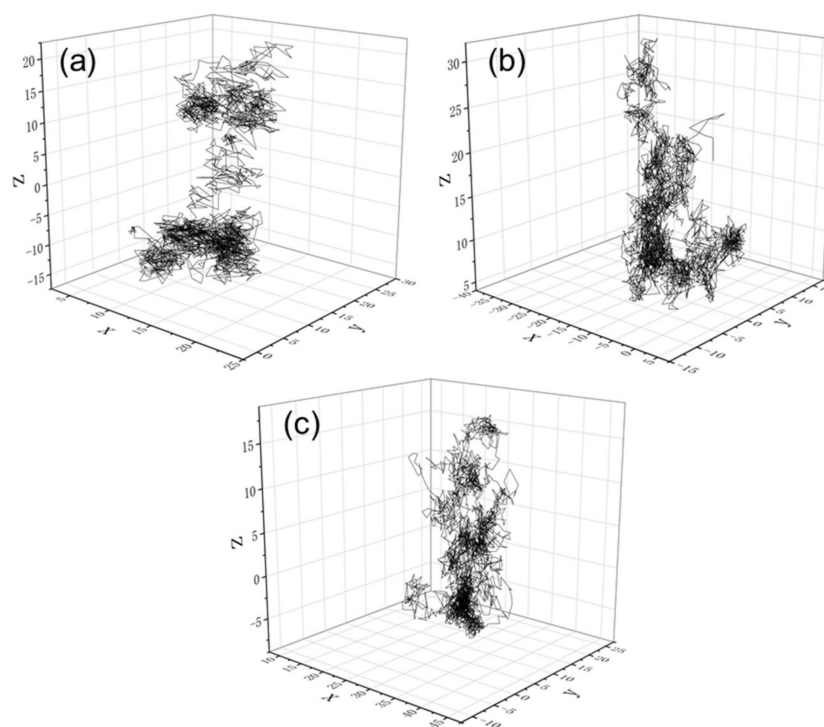


Figure 6. Trajectories of the three gases in PDMS membranes at 298 K: (a) N_2 (b) C_3H_8 and (c) C_3H_6 .

Figure 7 shows the adsorption isotherms of all three gases on the PDMS membrane at 298 K. At the same temperature and pressure, the number of gas molecules adsorbed by PDMS decreases in the order of C_3H_6 , C_3H_8 and N_2 . With an increase in pressure, the number of molecules adsorbed on the PDMS membrane gradually increases. When the pressure reaches 200 kPa, C_3H_8 and C_3H_6 reach the adsorption equilibrium, and the number of adsorbed molecules remains unchanged. However, N_2 does not reach the adsorption equilibrium, even as the pressure reaches 1000 kPa. This is because interactions of N_2 with PDMS chains are rather limited, compared to those of C_3H_8 and C_3H_6 . Even at lower pressure, PDMS can absorb sufficient C_3H_8 and C_3H_6 and reach equilibrium, but for N_2 , at pressures as high as 1000 kPa, we can observe that the amount of N_2 absorbed is still low and that there are still spaces in PDMS for more N_2 . As a result, an equilibrium is not reached.

Figure 8 shows the adsorption isotherms of all three gases in the PDMS membrane at different temperatures. At the same pressure, as the temperature increases, the number of adsorbed molecules for all three gases on the PDMS membrane decreases. As a result, though N_2 molecules are smaller, the number of molecules adsorbed is lower than for both C_3 molecules. This is contrary to the case of diffusivities. Smaller N_2 molecules have higher diffusivities than both C_3 molecules.

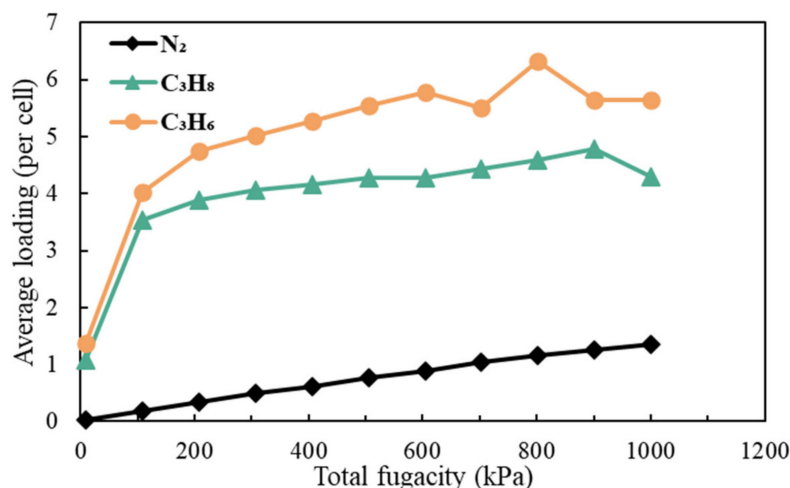


Figure 7. Adsorption isotherms of different gases on the PDMS membrane at 298 K.

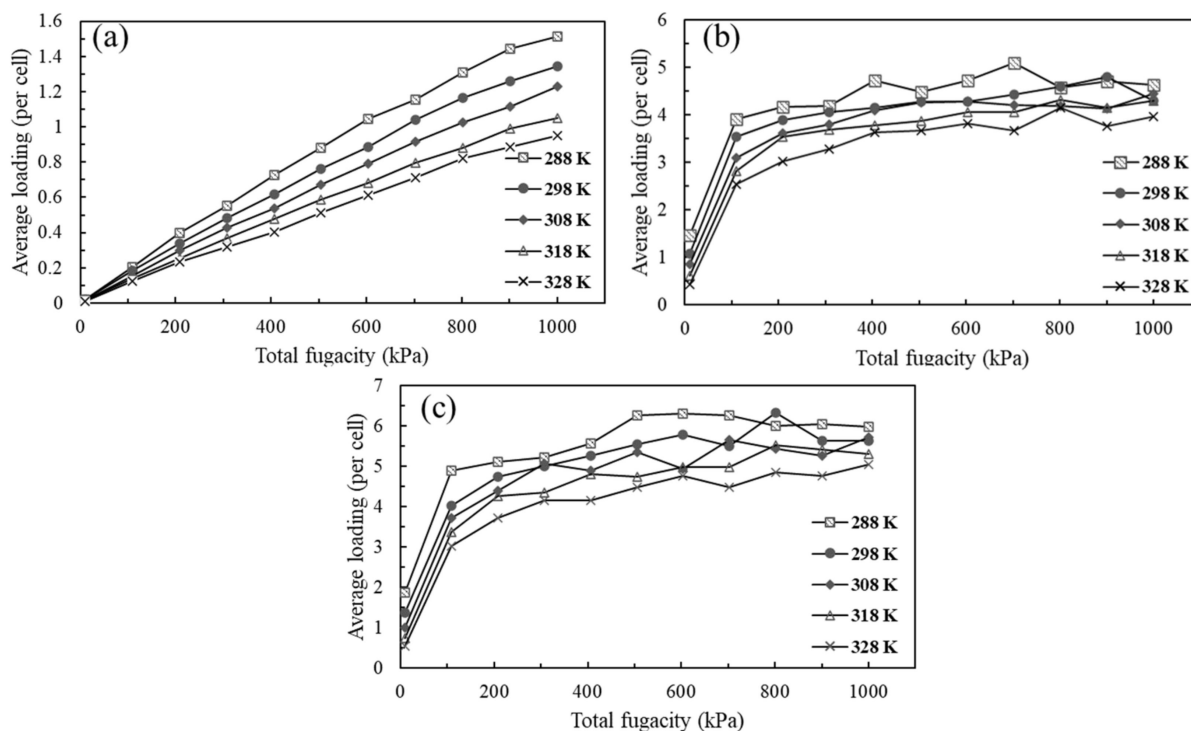


Figure 8. Adsorption isotherm of (a) N₂, (b) C₃H₈ and (c) C₃H₆ in PDMS membranes at different temperatures.

The solubility coefficients for the three gases, as pure gases and as mixed gases, in PDMS at 298 K are shown in Table 4. The competitive adsorption of gases in mixtures leads to a decrease in the solubility coefficients, and the decrease in the solubility coefficient of C₃ is greater than that of N₂.

Table 4. Solubility coefficients for the three gases as pure gases and as mixed gases in PDMS at 298 K.

Pure Gas	$S \times 10^2/\text{cm}^3 (\text{cm}^3 \cdot \text{cmHg})^{-1}$	Mixed Gas	$S \times 10^2/\text{cm}^3 (\text{cm}^3 \cdot \text{cmHg})^{-1}$
N ₂	0.22	N ₂	0.13
C ₃ H ₈	12.89	C ₃ H ₈	4.15
C ₃ H ₆	15.88	C ₃ H ₆	5.65

Figure 9 shows the solubility coefficients of N₂, C₃H₈ and C₃H₆ in the PDMS membranes at different temperatures. It can be observed that the solubility coefficients of C₃H₈ and C₃H₆ are relatively similar, while the solubility coefficient of N₂ in PDMS is much smaller than those of C₃H₈ and C₃H₆. This is consistent with the previous inference based on adsorption energy. The solubility coefficients of all three gases in PDMS gradually decrease as the temperature increases. Thus, we can observe that C₃ shows higher solubility than N₂. The most probable explanation for this is that C₃ has a higher transport rate in PDMS.

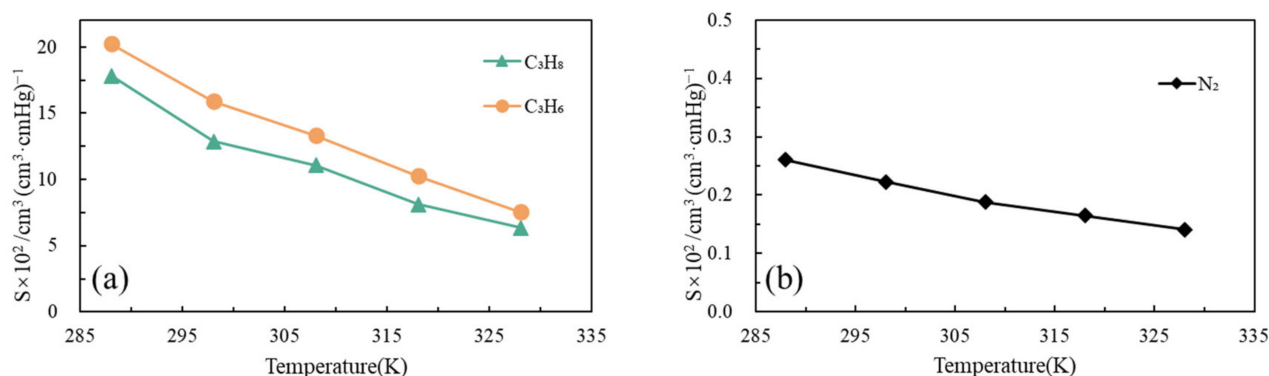


Figure 9. Solubility coefficients of (a) C₃ and (b) N₂ in the PDMS membranes at different temperatures.

The permeability coefficient can be calculated by multiplying the diffusion coefficient and solubility coefficient of gas in the PDMS membrane. Table 5 shows the permeability and selectivity coefficients of C₃/N₂ as pure gases and as mixed gases in the PDMS membrane. At 298 K, the selectivity coefficients of C₃/N₂ in PDMS are close to those obtained in the experimental results [27], and the selectivity coefficients of C₃/N₂ as mixtures are lower than those of C₃/N₂ as pure gases. Therefore, selectivity coefficients were obtained. This is the most important parameter to determine if a membrane can be used for the separation of gas mixtures.

Table 5. Permeability coefficients and selectivity coefficients of C₃/N₂ as pure gases and as mixed gases in PDMS at 298 K.

Pure Gas	P/Barrer	α _{C₃/N₂}	Mixed Gas	P/Barrer	α _{C₃/N₂}
N ₂	693	—	N ₂	403	—
C ₃ H ₈	14,621	21.10	C ₃ H ₈	8199	20.35
C ₃ H ₆	21,316	30.77	C ₃ H ₆	11,191	27.77

The permeability coefficients of the three gases at different temperatures are shown in Figure 10. The permeability coefficients of the two C₃ molecules in PDMS are similar to one another and are much higher than that of N₂. For the same gas, the permeability coefficient in PDMS decreases with an increase in temperature. The selectivity coefficient of C₃/N₂ gradually decreases with an increase in temperature.

According to the results, the apparently higher solubility coefficient of C₃ than that of N₂ results in higher permeability of C₃. Therefore, the transmembrane mass transfer of C₃ and N₂ in PDMS is mainly controlled by the dissolution step. Molecules with a large volume and low polarity, such as C₃, have high solubility in PDMS, and, thus, have a high permeability coefficient. This explains the unusual phenomena of large C₃ molecules having a higher transport rate than small N₂ molecules in PDMS.

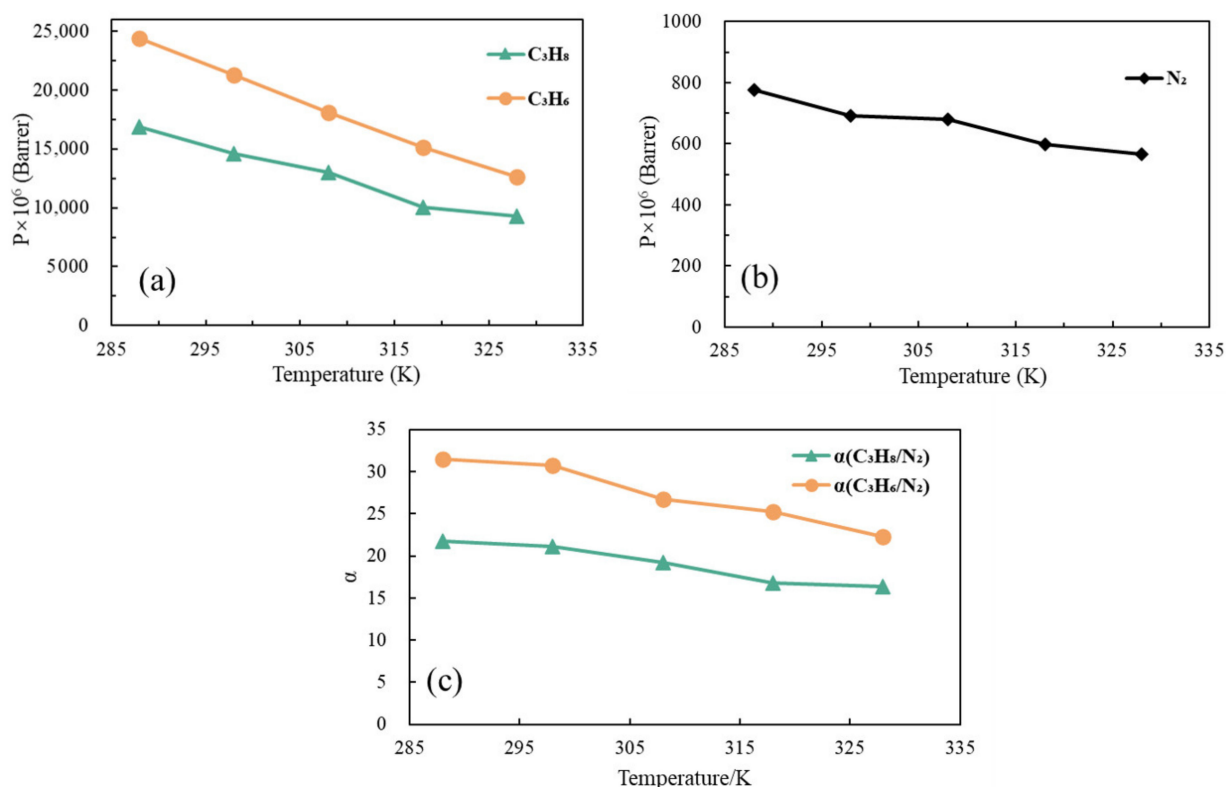


Figure 10. Permeability coefficients of (a) C₃ and (b) N₂, and (c) the selectivity coefficient of N₂, C₃H₈ and C₃H₆ at different temperatures.

4. Conclusions

In this study, the PDMS models were built using MS software, the related parameters of PDMS membranes were simulated, the transport process of C₃/N₂ in PDMS membranes was studied and analyzed, and the specific conclusions were as follows:

The diffusion and dissolution processes of C₃ and N₂ in PDMS membranes were analyzed using MD simulation and GCMC simulation, and the diffusion coefficient and solubility coefficient of C₃/N₂ in PDMS membranes were calculated. The results show that the diffusion rate of C₃ in PDMS membranes is lower than that of N₂, but the dissolution rate of C₃ in PDMS membranes is much greater than that of N₂, indicating that the mass transfer process of C₃ in PDMS membranes is mainly controlled by the dissolution process, while that of N₂ is mainly controlled by the diffusion process.

By comparing the mass transfer processes of pure gas and mixed gas, the effect of intermolecular force on the mass transfer process of gases in PDMS membranes was studied. It was found that under the same simulation conditions, the diffusion coefficients of gases in the mixed gas system are greater than those in the pure gas system, indicating that the diffusion process of gas molecules in polymer membranes has a synergistic effect. In the dissolution process, the solubility coefficients of various gases in the mixed gas system are lower than those of pure gases, indicating that there is a competitive adsorption relationship in the dissolution process of these gases in the PDMS membrane.

The effect of temperature on the mass transfer process of C₃/N₂ in PDMS membranes was also studied. The results show that with an increase in temperature from 288 K to 328 K, the diffusion coefficients of the three gases in PDMS gradually increase, the solubility coefficients gradually decrease, and the overall permeability selectivity coefficients of the gases gradually decrease. Therefore, according to an analysis of the control steps of the mass transfer of C₃/N₂ in PDMS membranes, it can be deduced that low-temperature conditions are more conducive to the separation of C₃/N₂ in PDMS membranes.

Supplementary Materials: The following are available online at <https://www.mdpi.com/article/10.3390/separations9050116/s1>, Figure S1. The relationship between the total energy and time in NVT ensemble.

Author Contributions: Data collation, W.C., M.W.; formal analysis, M.W. and G.Q.Y.; funding acquisition, W.C.; investigation, G.Q.Y. and M.W.; methodology, W.C., G.Q.Y. and Z.Z.; project management, W.C., G.Q.Y., Y.W. and J.L. All authors have read and agreed to the published version of the manuscript.

Funding: This work was supported by the National Natural Science Foundation of China (No. 21736001), the State Key Laboratory of Chemical Engineering (No. SKL-ChE-20A03), Fundamental Research Funds for the Central Universities (2021YJSHH16) and the Key Research and Development Program of Hebei Province (No. 21311101D).

Data Availability Statement: We will provide raw material upon the request of readers.

Conflicts of Interest: There are no conflicts of interest to declare.

References

1. Kamal, M.S.; Razzak, S.A.; Hossain, M.M. Catalytic oxidation of volatile organic compounds (VOCs)—A review. *Atmos. Environ.* **2016**, *140*, 117–134. [[CrossRef](#)]
2. Liu, B.Y.; Ji, J.; Zhang, B.G.; Huang, W.J.; Gan, Y.L.; Leung, D.Y.C.; Huang, H.B. Catalytic ozonation of VOCs at low temperature: A comprehensive review. *J. Hazard. Mater.* **2021**, *422*, 126847. [[CrossRef](#)] [[PubMed](#)]
3. Zhang, X.Y.; Gao, B.; Creamer, A.E.; Cao, C.C.; Li, Y.C. Adsorption of VOCs onto engineered carbon materials: A review. *J. Hazard. Mater.* **2017**, *338*, 102–123. [[CrossRef](#)] [[PubMed](#)]
4. Ren, Y.Q.; Wei, J.; Wang, G.H.; Wu, Z.H.; Ji, Y.Y.; Li, H. Evolution of aerosol chemistry in Beijing under strong influence of anthropogenic pollutants: Composition, sources, and secondary formation of fine particulate nitrated aromatic compounds. *Environ. Res.* **2022**, *204*, 111982. [[CrossRef](#)]
5. Bari, M.A.; Kindziarski, W.B. Ambient volatile organic compounds (VOCs) in Calgary, Alberta: Sources and screening health risk assessment. *Sci. Total Environ.* **2018**, *631–632*, 627–640. [[CrossRef](#)]
6. Dai, C.H.; Zhou, Y.Y.; Peng, H.; Huang, S.J.; Qin, P.F.; Zhang, J.C.; Yang, Y.; Luo, L.; Zhang, X.S. Current progress in remediation of chlorinated volatile organic compounds: A review. *J. Ind. Chem.* **2018**, *62*, 106–119.
7. Atthajariyakul, S.; Leephakpreeda, T. Real-time determination of optimal indoor-air condition for thermal comfort, air quality and efficient energy usage. *Energy Build.* **2004**, *36*, 720–733. [[CrossRef](#)]
8. Yang, Y.; Ji, D.; Sun, J.; Wang, Y.H.; Yao, D. Ambient volatile organic compounds in a suburban site between Beijing and Tianjin: Concentration levels, source apportionment and health risk assessment. *Sci. Total Environ.* **2019**, *695*, 133889. [[CrossRef](#)]
9. Ding, Y. Volatile Organic Compound Liquid Recovery by the Dead End Gas Separation Membrane Process: Theory and Process Simulation. *Ind. Eng. Chem. Res.* **2019**, *58*, 5008–5017. [[CrossRef](#)]
10. Belaissaoui, B.; Le Moullec, Y.; Favre, E. Energy efficiency of a hybrid membrane/condensation process for VOC (Volatile Organic Compounds) recovery from air: A generic approach. *Energy* **2016**, *95*, 291–302. [[CrossRef](#)]
11. Li, X.; Zhang, L.; Yang, Z.Q.; Wang, P.; Yan, Y.F.; Ran, J.Y. Adsorption materials for volatile organic compounds (VOCs) and the key factors for VOCs adsorption process: A review. *Sep. Purif. Technol.* **2020**, *235*, 116213. [[CrossRef](#)]
12. Bernardo, P.; Drioli, E.; Golemme, G. Membrane Gas Separation: A Review/State of the Art. *Ind. Eng. Chem. Res.* **2009**, *48*, 4638–4663. [[CrossRef](#)]
13. Yang, W.C.; Zhou, H.L.; Zong, C.X.; Li, Y.X.; Jin, W.Q. Study on membrane performance in vapor permeation of VOC/N₂ mixtures via modified constant volume/variable pressure method. *Sep. Purif. Technol.* **2018**, *200*, 273–283. [[CrossRef](#)]
14. Şahin, F.; Topuz, B.; Kalıpçılar, H. ZIF filled PDMS mixed matrix membranes for separation of solvent vapors from nitrogen. *J. Membr. Sci.* **2020**, *598*, 117792. [[CrossRef](#)]
15. Gazic, F.R.; Saljoughi, E.; Mousavi, S.M. Recovery of 1-ethyl-2-methylbenzene from wastewater by polymeric membranes via pervaporation process. *J. Polym. Res.* **2019**, *26*, 272. [[CrossRef](#)]
16. Kim, H.J.; Nah, S.S.; Min, B.R. A new technique for preparation of PDMS pervaporation membrane for VOC removal. *Adv. Environ. Res.* **2002**, *6*, 255–264. [[CrossRef](#)]
17. Shi, Y.T.; Burns, C.; Feng, X.S. Poly (dimethyl siloxane) thin film composite membranes for propylene separation from nitrogen. *J. Membr. Sci.* **2006**, *282*, 115–123. [[CrossRef](#)]
18. Cai, W.B.; Xie, J.Y.; Luo, J.Y.; Chen, X.H.; Wang, M.Q.; Wang, Y.J.; Li, J.D. n-Octyltrichlorosilane Modified SAPO-34/PDMS Mixed Matrix Membranes for Propane/Nitrogen Mixture Separation. *Separations* **2022**, *9*, 64. [[CrossRef](#)]
19. Liu, C.L.; Ding, C.; Hao, X.G.; Li, C.C.; An, X.W.; Wang, P.F.; Zhang, B.L.; Gao, F.L.; Peng, C.J.; Guan, G.Q. Molecular dynamics simulation and experimental investigation of furfural separation from aqueous solutions via PEBA-2533 membranes. *Sep. Purif. Technol.* **2018**, *207*, 42–50. [[CrossRef](#)]

20. Pazirofteh, M.; Dehghani, M.; Niazi, S.; Mohammadi, A.H.; Asghari, M. Molecular dynamics simulation and Monte Carlo study of transport and structural properties of PEBA 1657 and 2533 membranes modified by functionalized POSS-PEG material. *J. Mol. Liq.* **2017**, *241*, 646–653. [[CrossRef](#)]
21. Wang, H.Y.; Liu, C.L.; Xu, Q.; Du, X.; Li, C.C.; Gao, F.F.; Hao, X.G.; Peng, C.J.; Guan, G.Q. Swelling mechanism of PEBA-2533 membrane for pervaporation separation of high boiling point organic compounds: Experiment and molecular dynamics simulation. *Sep. Purif. Technol.* **2020**, *2452*, 116851. [[CrossRef](#)]
22. Zuo, C.Y.; Tu, R.; Ding, X.B.; Xing, W.H. Recovery of isobutanol from esterified wastewater by PDMS composite membrane. *CIESC J.* **2020**, *71*, 4189–4199.
23. Lue, S.J.; Jia, S.O.; Chen, S.L.; Hung, W.S.; Hu, C.C.; Jean, Y.C.; Lai, J.Y. Tailoring permeant sorption and diffusion properties with blended polyurethane/poly(dimethylsiloxane) (PU/PDMS) membranes. *J. Membr. Sci.* **2010**, *356*, 78–87. [[CrossRef](#)]
24. Ramirez-Gutierrez, D.; Nieto-Draghi, C.; Pannacci, N.; Castro, L.V.; Alvarez-Ramirez, F.; Creton, B. Surface Photografting of Acrylic Acid on Poly(dimethylsiloxane). Experimental and Dissipative Particle Dynamics Studies. *Langmuir* **2015**, *31*, 1400–1409. [[CrossRef](#)]
25. Huang, J.C. Estimation of solubility parameter components of solutes and polymers using heat of vaporization and heat of sorption of solutes. *J. Appl. Polym. Sci.* **2010**, *112*, 2027–2032. [[CrossRef](#)]
26. Wu, Y.Q.; Liu, X.M. Arrhenius relationship and two-step scheme in AF hyperdynamics simulation of diffusion of Mg/Zn in-interface. *Trans. Nonferrous Metal. Soc.* **2013**, *23*, 508–516. [[CrossRef](#)]
27. Fang, M.Q.; Wu, C.L.; Yang, Z.J.; Wang, T.; Xia, Y.; Li, J.D. ZIF-8/PDMS mixed matrix membranes for propane/nitrogen mixture separation: Experimental result and permeation model validation. *J. Membr. Sci.* **2015**, *474*, 103–113. [[CrossRef](#)]